Journal of Biophotonics

JOURNAL OF BIOPHOTONICS

RESEARCH ARTICLE

Noncontact Detection of Blood Coagulation Dynamics Based on Speckle Deviation Analysis Using Optical Coherence Tomography

Yun Tang[1,2] | Zongqing Ma[1] | Yuxian Zhang[1] | Fan Fan[1] | Fan Zhang[1] | Jiang Zhu[1]

[1]Key Laboratory of the Ministry of Education for Optoelectronic Measurement Technology and Instrument, Beijing Information Science and Technology University, Beijing, China | [2]State Key Laboratory of Extreme Photonics and Instrumentation, College of Optical Science and Engineering, Zhejiang University, Hangzhou, Zhejiang, China

Correspondence: Zongqing Ma (zqma@bistu.edu.cn) | Jiang Zhu (jiangzhu@bistu.edu.cn)

Received: 31 December 2024 | **Revised:** 11 February 2025 | **Accepted:** 24 February 2025

Funding: This work was supported by Research Project of Beijing Municipal Education Commission (KM202311232021) and National Natural Science Foundation of China (52475546, 52205551).

Keywords: blood coagulation | optical coherence tomography | speckle deviation analysis | viscosity

ABSTRACT

Red blood cells aggregate from individual cells into larger aggregates during blood coagulation. This process causes the light-scattering particles to enlarge and their motion to become restricted. The size and motion of these light-scattering particles during coagulation provide valuable information on the progress of blood coagulation. This paper proposes an optical coherence tomography speckle deviation (OCT-SD) method for the noncontact assessment of blood coagulation dynamics by detecting changes in the size and motion of scattering particles. The coagulation characteristics of static and flowing blood were quantitatively evaluated through coagulation reaction time and clot formation duration by monitoring the blood coagulation process. The OCT imaging, incorporating SD analysis, enables noncontact coagulation assessment. Experimental results demonstrate that the proposed method can efficiently and accurately assess coagulation dynamics, offering significant potential for in situ coagulation detection.

1 | Introduction

A coagulation disorder refers to an abnormal state of blood clotting and bleeding. Coagulation assessment plays a crucial role in predicting the risks associated with such disorders and identifying their underlying causes. Coagulation properties are typically analyzed through biochemical and physical testing [1, 2]. In biochemical testing, the quantity or activity of various coagulation factors in the blood is measured. However, these tests often involve complex sample pretreatment and are time-consuming. Physical testing methods—such as light absorption/scattering detection or blood viscoelasticity measurements—offer more efficient coagulation assessments with minimal sample preparation. These methods are, therefore, promising for point-of-care testing.

As a label-free, noncontact imaging technology, optical coherence tomography (OCT) has been widely applied in three-dimensional ophthalmic imaging, endoscopy, and angiography [3–5]. OCT signal decay with depth has been utilized to monitor the coagulation process by detecting changes in optical parameters, such as scattering coefficients and refractive indices, during coagulation [6, 7]. However, the optical properties of blood can also be altered by certain conditions, such as lipemia or icterus, potentially leading to distorted coagulation evaluations. Like thromboelastography (TEG) and rotational thromboelastometry (ROTEM), optical coherence elastography combines the principles of elastography with OCT to monitor blood coagulation by assessing blood viscoelasticity [8–10]. This technique calculates shear wave velocity and compressional wave attenuation

to evaluate blood viscoelasticity after mechanical waves are induced by external excitation. However, viscoelasticity-based coagulation detection requires additional force excitation devices and sophisticated operational procedures.

This study proposes an OCT speckle deviation (OCT-SD) method for evaluating blood coagulation properties. By analyzing the SD of time-series OCT signals, changes in the size and motion of scattering particles can be detected. We investigated the relationship between OCT-SDs and particle size and motion in polystyrene microsphere suspensions. Subsequently, we monitored blood coagulation under both static and dynamic conditions, quantifying coagulation reaction time and clot formation duration in coagulation activation, blood dilution, and flowing blood assays.

2 | Methods and Materials

2.1 | OCT-SD Analysis

The composition and properties of blood are crucial to its rheology and coagulation function [11, 12]. Red blood cells (RBCs), which account for over 99% of the blood cell volume [13], are the primary light-scattering particles in the blood. The biconcave, disc-shaped RBC has an elastic membrane enclosing a hemoglobin solution, which allows it to deform [14]. During blood coagulation, RBCs aggregate as fibrin networks form, binding the cells together [15]. As a result, the light-scattering particles increase in size from individual RBCs to RBC aggregates. Additionally, RBC aggregation raises blood viscosity and restricts the motion of scattering particles. Consequently, the blood coagulation process can be monitored by detecting changes in both the size and motion of scattering particles, as shown in Figure 1. In the early stage of coagulation, individual RBCs dominate as scattering particles in low-viscosity blood, resulting in small particle size and rapid motion. In the later stages, large RBC aggregates take over as the primary scattering particles in high-viscosity blood, causing the motion to slow down.

Built upon the principle of low-coherence interferometry, OCT captures optical scattering signals at high speed and resolution, enabling depth profiling. The SD of time-series OCT signals is highly sensitive to the size and motion of scattering particles. Changes in particle size can lead to significant variations in the standard deviation, with smaller particles causing a larger SD [16]. Additionally, the motion of the scattering particles influences the SD, with faster motion resulting in a higher standard deviation value [17]. The SD of time-series OCT signals can be calculated using the following equation:

$$\beta_S = \sqrt{\frac{\sum_{m=1}^{M}\left[I(m)-\bar{I}\right]^2}{M-1}} \tag{1}$$

where β_s is the SD, M denotes the number of speckle regions in an M-scan image, $I(m)$ represents the average amplitude of the mth speckle region, and $\bar{I}$ is calculated by $\frac{1}{M}\times\sum_{m=1}^{M} I(m)$. In a blood sample, the SD is primarily influenced by the size of the particles and their random motion. During coagulation, the dominant scattering particles increase in size, transitioning from individual RBCs to RBC aggregates, and the random motion slows down due to the formation and binding of fibrin networks. Larger scattering particles with slower random motion lead to a decrease in SD. As a result, the coagulation process can be monitored through SD analysis. Calculating SDs is simpler than performing autocorrelation analysis [11], making it a valuable method for real-time coagulation detection.

2.2 | Data Capture

OCT signals were acquired using a Thorlabs swept-source OCT system (VEG210C1) with a central wavelength of 1300 nm and an A-scan speed of 100 kHz, as shown in Figure 2. An M-scan image, consisting of 10,000 A-scans and 512 depth spots, was captured at each time point. A 15 × 15 pixel region in the M-scan image was selected as the speckle region, and 666 such speckle regions were defined at specific depths within the M-scan. Therefore, the total number of speckle regions (M) was 666, with a time interval of 0.15 ms between adjacent regions.

2.3 | Sample Preparation

To validate the feasibility of our method, we measured suspensions of polystyrene microspheres with diameters of 5, 20, and 100 μm dispersed in water. RBCs with a size of approximately 5–10 μm and their aggregates (much larger than individual cells) significantly influence the scattering properties during OCT measurements. To consider these effects, we measured 5–100 μm microsphere suspensions using OCT. A 1-mL sample of the microsphere suspension was gently shaken in a centrifuge tube to ensure uniform mixing. Additionally, suspensions with varying viscosities were compared by adding glycerin to the solution. Three suspensions with 5 μm microspheres were

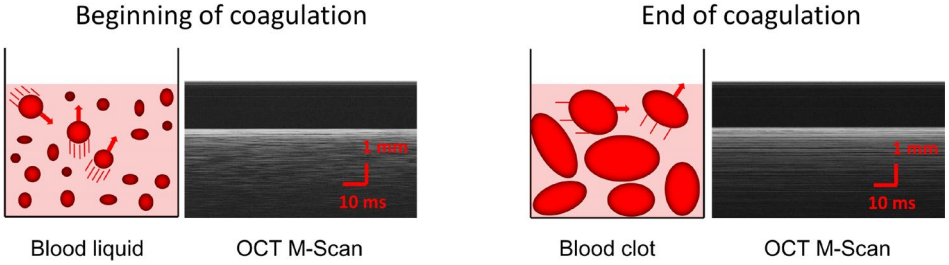

FIGURE 1 | Schematic of OCT speckle deviation analysis. In the early stage of coagulation, individual RBCs are the dominant scattering particles, while in the later stages, large RBC aggregates become the primary scattering particles.

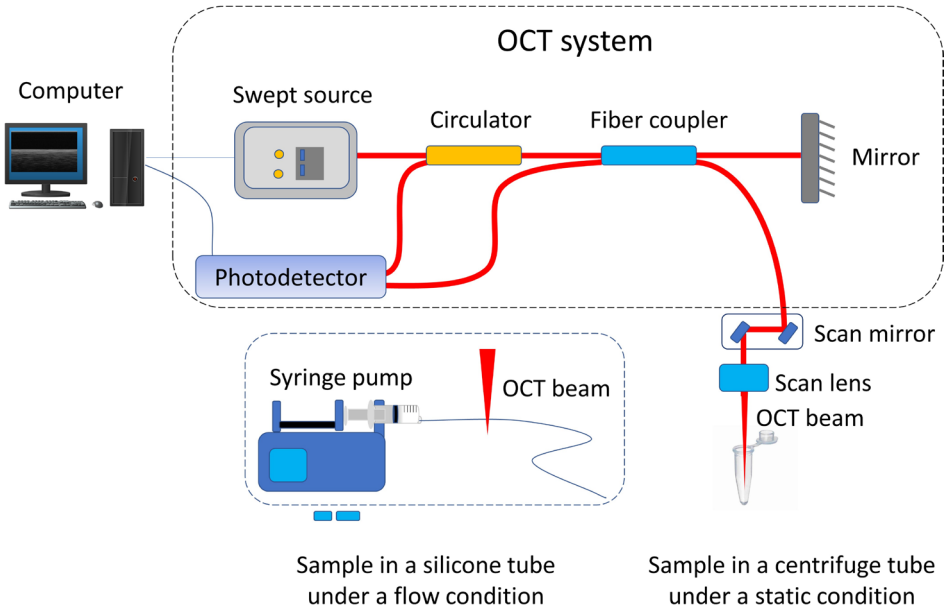

FIGURE 2 | Schematic of the system for detecting blood coagulation dynamics. A swept-source OCT system was used to capture OCT signals from the sample in a centrifuge tube under static conditions, or from the sample in a silicone tube under flow conditions.

tested, including samples without glycerin, with 16% glycerin, and with 34% glycerin. Thirty frames of M-scan OCT images were captured for each sample as repeated measurements.

Porcine blood is commonly used in coagulation studies [18]. Fresh porcine whole blood was anticoagulated with sodium citrate and recalcified with a $CaCl_2$ solution to trigger coagulation. Two assays were designed: the ellagic acid (EA) activation assay and the sodium chloride dilution assay. In the EA activation assay, 2.5 mL of the blood sample was mixed with 100 μL (10 g/L) of the EA solution and 145 μL (12 g/L) of the $CaCl_2$ solution. The EA accelerates coagulation. In the NaCl dilution assay, whole blood samples were diluted to 75% and 50% with a 0.9% NaCl solution. Then, 2.5 mL of each diluted blood sample was mixed with 100 μL (10 g/L) of the EA solution and 145 μL (12 g/L) of the $CaCl_2$ solution. Each sample was gently mixed for 30 s, followed by pipetting 1 mL of the mixture into a centrifuge tube for testing under static conditions. To monitor blood coagulation under flow conditions, 2.5 mL of the blood sample, as in the EA activation assay, was injected into a 1 mm silicone tube. The blood was cycled reciprocally in the tube: forward flow for 6 s, a 6 s pause, and reverse flow for 6 s, controlled by a syringe pump. Two blood flow rates (1 mL/min and 2 mL/min) were tested in the experiments. Three replicate measurements were performed for each sample group. Speckle variance is also sensitive to factors such as blood flow velocity. As a result, when measuring speckle variances under flow conditions, the flow was temporarily paused.

3 | Results

The OCT-SD measurements of polystyrene microsphere suspensions are shown in Figure 3. Figure 3a illustrates the OCT M-scan images of suspensions containing microspheres with diameters of 5, 20, and 100 μm. Figure 3b presents the SDs for the three sample groups. As observed, when the microsphere diameter increases from 5 to 20 μm, the SD β_s decreases significantly from 55.81 ± 1.55 to 39.28 ± 1.67 ($p < 0.01$). A further increase in microsphere diameter to 100 μm results in a β_s value of 9.01 ± 0.28 ($p < 0.01$). A strong correlation is observed between the microsphere size and the SD, as analyzed using the OCT-SD method.

The OCT-SD measurements of 5-μm microsphere suspensions with varying viscosities are shown in Figure 3c. The viscosity of the suspensions was measured using a rotational rheometer (Physica MCR301, Anton Paar, Graz, Austria). The viscosity values were 1 mPa s for pure water, 149 mPa s for a mixture with 16% glycerol, and 450 mPa s for a mixture with 34% glycerol. As shown in Figure 3c, when the viscosity of the medium increases, the SD decreases significantly, from 55.81 ± 1.55 for the sample without glycerol to 22.13 ± 0.60 for the sample with 16% glycerol ($p < 0.01$). It further decreases to 14.92 ± 0.40 for the sample with 34% glycerol ($p < 0.01$). A strong correlation is observed between sample viscosity and SD, as analyzed by the OCT-SD method.

During coagulation, both particle size and viscosity change simultaneously, with the two factors having an additive effect rather than canceling each other out. Specifically, as coagulation progresses, the primary scattering particles transition from smaller RBCs in low-viscosity blood to larger red blood cell aggregates in high-viscosity blood. As particle size increases, SD decreases, and as viscosity increases, SD also decreases. Therefore, SD can be used to detect coagulation as it progresses.

Blood coagulation was analyzed using the OCT-SD method under both static and flow conditions, as shown in Figure 4. During coagulation, as fibrin networks form and bind RBCs, the scattering particles increase in size, and their motion slows down, resulting in a decrease in SD. Figure 4a illustrates the changes in SD after coagulation was triggered in static blood samples. The coagulation process consists of three main stages. In the first stage, individual RBCs are suspended in liquid blood. The scattering particles are small, and their random

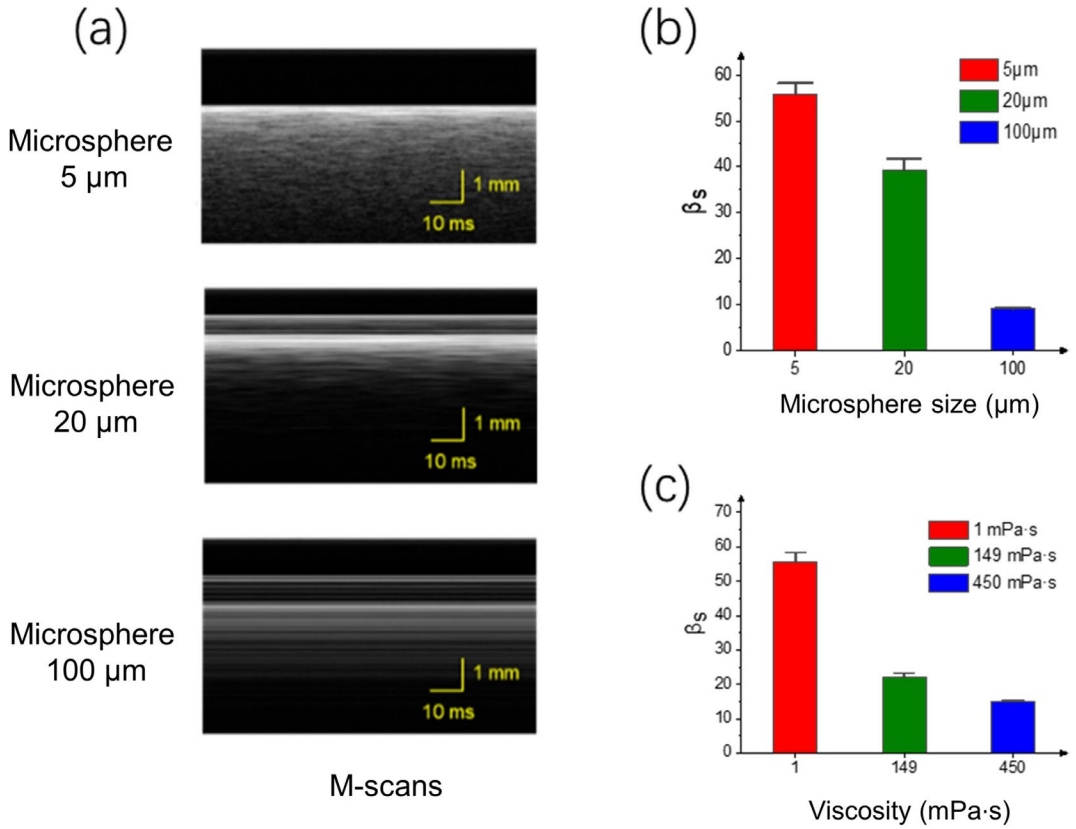

FIGURE 3 | OCT-SD measurements of polystyrene microsphere suspensions with varying diameters and viscosities. (a) OCT M-scan images of the microsphere suspensions. (b) Speckle deviations for water suspensions with different microsphere diameters. (c) Speckle deviations for 5 μm microsphere suspensions with varying viscosities.

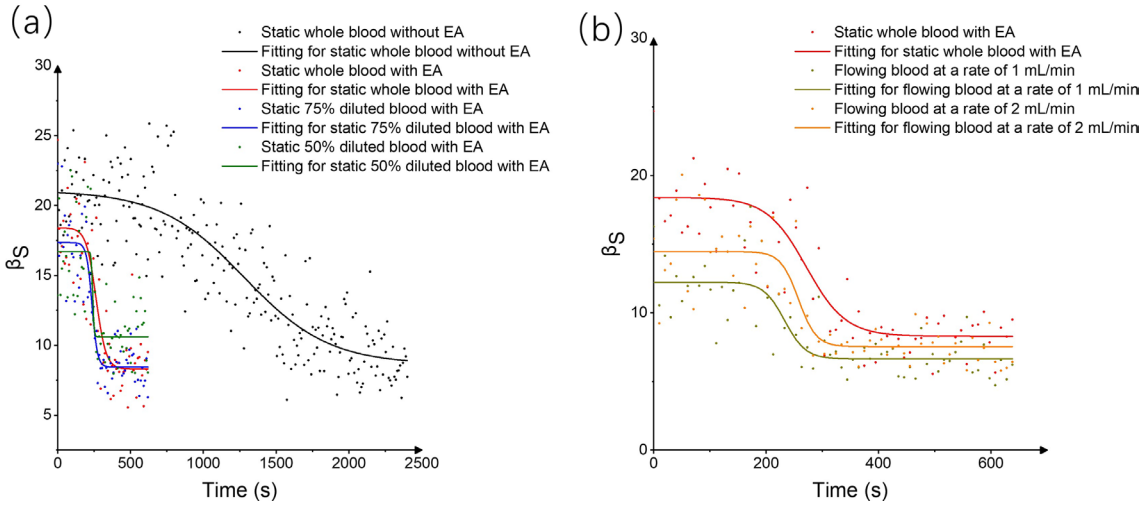

FIGURE 4 | Analysis of speckle deviation β_s during blood coagulation. (a) Speckle deviations for static whole blood and static diluted blood samples. (b) Speckle deviations for static blood and flowing blood samples.

motion is rapid, leading to a high SD. In the second stage, the liquid blood quickly transforms into a gel clot. As RBCs aggregate into clusters through fibrin network binding, the particle size gradually increases, and the motion of the aggregates slows down. This results in a gradual decrease in SD. In the third stage, fibrin networks intertwine with the RBCs, forming a stable blood clot [19]. At this point, the size and motion of the scattering particles no longer change significantly, and the SD stabilizes. Based on the three stages of blood clotting, the SDs were fitted to an S-curve, and the second-order derivatives were calculated. Coagulation properties were then analyzed using two metrics: coagulation reaction time and clot formation duration. The coagulation reaction time, defined as the point at which coagulation begins, is determined by the time at which the minimum value of the second-order derivative occurs. The clot formation duration, representing the period during

clot formation, is calculated as the time interval between the minimum and maximum values of the second-order derivatives. These two metrics—coagulation reaction time and clot formation duration—are compared in Table 1. Various factors, including sample properties and OCT system settings, can influence SD, resulting in differences at the onset of coagulation and fluctuations during coagulation measurements, as shown in Figure 4. However, since the SDs are fitted to an S-curve and second-order derivatives are used to assess coagulation, any fluctuations in the measurements do not significantly impact the measurement accuracy of coagulation reaction time and clot formation duration. To improve measurement accuracy, it is possible to increase the sliding window size and the number of averaging times within the OCT-SD algorithm, although this will also raise the computational cost.

The proposed OCT-SD method was evaluated under static conditions using the EA activation and NaCl dilution assays. EA is an organic compound that activates the contact phase of the intrinsic coagulation pathway, accelerating the coagulation process [20]. The NaCl dilution of blood during infusion therapy can lead to dilutional coagulopathy, affecting coagulation properties [21]. Figure 4a compares the SDs among four static blood samples: whole blood without EA, whole blood with EA, 75% diluted blood with EA, and 50% diluted blood with EA. The measurement time was shorter for samples with EA compared to those without EA, as EA significantly accelerated the coagulation process. The coagulation reaction time and clot formation duration for the static samples are compared in Table 1.

After the addition of EA, the coagulation reaction time decreased significantly from 972 ± 46 to 271 ± 15 s ($p < 0.05$), and the clot formation duration significantly shortened from 645 ± 74 to 101 ± 13 s ($p < 0.05$). These results confirm that EA can promote blood coagulation [22]. The effect of NaCl hemodilution on coagulation was assessed in three static samples with EA. Hemodilution did not significantly affect the coagulation reaction time ($p > 0.05$), indicating that coagulation began almost simultaneously across the samples. However, the clot formation duration significantly decreased from 101 ± 13 s for whole blood to 42 ± 12 s for 75% diluted blood ($p < 0.05$) and further reduced to 24 ± 14 s for 50% diluted blood ($p < 0.05$). This suggests that hemodilution accelerates the coagulation process, leading to faster clot formation [23].

We also assessed the effects of flow rates on coagulation. EA samples were driven to flow reciprocally at flow rates of 1 mL/min and 2 mL/min, respectively. The corresponding SDs for the flowing blood samples are shown in Figure 4b. A comparison of the coagulation property metrics is presented in Table 1. There was no significant difference in coagulation reaction time between static whole blood with EA and flowing blood with EA at either 1 mL/min ($p > 0.05$) or 2 mL/min ($p > 0.05$). However, the clot formation duration was significantly shortened from 101 ± 13 s for static whole blood to 35 ± 13 s for flowing blood at 1 mL/min ($p < 0.05$) and further reduced to 24 ± 14 s for flowing blood at 2 mL/min ($p < 0.05$). These results suggest that blood flow accelerates the formation of fibrin networks and promotes RBC aggregation after coagulation initiation, as observed from the OCT-SD analysis.

TABLE 1 | Coagulation properties of static blood and flow blood.

Blood sample	Coagulation reaction time (s)	Clot formation duration (s)
Static whole blood without EA	972 ± 46	645 ± 74
Static whole blood with EA	271 ± 15	101 ± 13
Static 75% diluted blood with EA	217 ± 7	42 ± 12
Static 50% diluted blood with EA	231 ± 6	24 ± 14
Whole blood with EA at 1 mL/min	245 ± 17	35 ± 13
Whole blood with EA at 2 mL/min	255 ± 13	24 ± 14

4 | Conclusions

In this work, we proposed an OCT-SD method for noncontact blood coagulation detection. The changes in the size and the motion of the scattering particles during the coagulation were evaluated by calculating the SDs of time-series OCT signals. As only OCT images are required for the SD analysis, the OCT-SD method provides a noncontact coagulation assessment and could be used for in situ coagulation monitoring. Another advantage of the proposed OCT-SD method is its relatively low runtime cost due to the simple calculation of the SDs. The OCT-SD analysis simplifies the calculations and increases the efficiency, which is essential for point-of-care testing. The experimental results demonstrate that the proposed method can accurately characterize the coagulation properties in static and flow conditions. Therefore, the proposed OCT-SD method holds the potential for real-time in situ coagulation detection.

Conflicts of Interest

The authors declare no conflicts of interest.

Data Availability Statement

The data that support the findings of this study are available from the corresponding author upon reasonable request.

References

1. M. Mohammadi Aria, A. Erten, and O. Yalcin, "Technology Advancements in Blood Coagulation Measurements for Point-Of-Care Diagnostic Testing," *Frontiers in Bioengineering and Biotechnology* 7 (2019): 395.

2. K. Naseer, S. Ali, and J. Qazi, "ATR-FTIR Spectroscopy as the Future of Diagnostics: A Systematic Review of the Approach Using Bio-Fluids," *Applied Spectroscopy Reviews* 56, no. 2 (2021): 85–97.

3. C. Yang, J. Zhu, L. Zhu, et al., "Rapid Estimations of Intensity Standard Deviations for Optical Coherence Tomography Angiography," *Journal of Biophotonics* 15, no. 4 (2022): e202100340.

4. L. Hu, R. Guo, S. Li, et al., "Accuracy Improvement for Classifying Retinal OCT Images by Diseases Using Deep Learning-Based Selective Denoising Approach," *Journal of Innovative Optical Health Sciences* 16, no. 6 (2023): 2350008.

5. C. Niu, Z. Guan, H. Yu, et al., "Endoscopic OCTA in Continuous Rotation and Retraction Scheme Using a Proximal Scanning Catheter," *Optics Express* 32, no. 19 (2024): 32799.

6. X. Xu, J. Lin, and F. Fu, "Optical Coherence Tomography to Investigate Optical Properties of Blood During Coagulation," *Journal of Biomedical Optics* 16, no. 9 (2011): 096002.

7. X. Xu, J. Geng, and X. Teng, "Monitoring the Blood Coagulation Process Under Various Flow Conditions With Optical Coherence Tomography," *Journal of Biomedical Optics* 19, no. 4 (2014): 046021.

8. J. Zhu, X. He, and Z. Chen, "Acoustic Radiation Force Optical Coherence Elastography for Elasticity Assessment of Soft Tissues," *Applied Spectroscopy Reviews* 54, no. 6 (2019): 457–481.

9. X. Xu, J. Zhu, and Z. Chen, "Dynamic and Quantitative Assessment of Blood Coagulation Using Optical Coherence Elastography," *Scientific Reports* 6 (2016): 24294.

10. X. Xu, J. Zhu, J. Yu, et al., "Viscosity Monitoring During Hemodiluted Blood Coagulation Using Optical Coherence Elastography," *IEEE Journal of Selected Topics in Quantum Electronics* 25, no. 1 (2019): 7200406.

11. Y. Tang, J. Zhu, L. Zhu, et al., "Blood Coagulation Monitoring Under Static and Flow Conditions With Optical Coherence Tomography Autocorrelation Analysis," *Applied Physics Letters* 120 (2022): 163702.

12. F. Yilmaz and M. Y. Gundogdu, "A Critical Review on Blood Flow in Large Arteries; Relevance to Blood Rheology, Viscosity Models, and Physiologic Conditions," *Korea-Australia Rheology Journal* 20, no. 4 (2008): 197–211.

13. C. Picart, J. M. Piau, H. Galliard, and P. Carpentier, "Human Blood Shear Yield Stress and Its Hematocrit Dependence," *Journal of Rheology* 42, no. 1 (1998): 1–12.

14. P. Snabre and P. Mills, "Rheology of Weakly Flocculated Suspensions of Viscoelastic Particles," *Journal de Physique III France* 6, no. 12 (1996): 1835–1855.

15. A. L. Zydney, "A Constitutive Equation for the Viscosity of Stored Red Cell Suspensions: Effect of Hematocrit, Shear Rate, and Suspending Phase," *Journal of Rheology* 35, no. 8 (1991): 1639–1680.

16. M. Almasian, T. G. van Leeuwen, and D. J. Faber, "OCT Amplitude and Speckle Statistics of Discrete Random Media," *Scientific Reports* 7, no. 1 (2017): 14873.

17. J. Zhu, X. He, and Z. Chen, "Perspective: Current Challenges and Solutions of Doppler Optical Coherence Tomography and Angiography for Neuroimaging," *APL Photonics* 3 (2018): 120902.

18. J. L. Sondeen, R. de Guzman, I. A. Polykratis, et al., "Comparison Between Human and Porcine Thromboelastograph Parameters in Response to Ex-Vivo Changes to Platelets, Plasma, and Red Blood Cells," *Blood Coagulation & Fibrinolysis* 24, no. 8 (2013): 818–829.

19. A. C. Swanepoel, V. G. Nielsen, and E. Pretorius, "Viscoelasticity and Ultrastructure in Coagulation and Inflammation: Two Diverse Techniques, One Conclusion," *Inflammation* 38, no. 4 (2015): 1707–1726.

20. G. Lima-Oliveira, L. M. Brennan-Bourdon, B. Varela, et al., "Clot Activators and Anticoagulant Additives for Blood Collection. A Critical Review on Behalf of COLABIOCLI WG-PRE-LATAM," *Critical Reviews in Clinical Laboratory Sciences* 58, no. 3 (2021): 207–224.

21. B. Liu, Y. Liu, H. Wei, et al., "Effects of Haemodilution on the Optical Properties of Blood During Coagulation Studied by Optical Coherence Tomography," *Quantum Electronics* 46, no. 11 (2016): 1055–1060.

22. L. Gopalakrishnan, L. N. Ramana, S. Sethuraman, and U. M. Krishnan, "Ellagic Acid Encapsulated Chitosan Nanoparticles as Anti-Hemorrhagic Agent," *Carbohydrate Polymers* 111 (2014): 215–221.

23. S. M. Bertoluzzo, A. Bollini, M. Rasia, and A. Raynal, "Kinetic Model for Erythrocyte Aggregation," *Blood Cells, Molecules & Diseases* 25, no. 6 (1999): 339–349.